

A Generalized Approach to Relaxation Time of Magnetic Nanoparticles With Interactions: From Superparamagnetic Behavior to Spin-Glass Transition

Jean Claudio Cardoso Cerbino¹ and Diego Muraca^{1,*}

¹ “Gleb Wataghin” Institute of Physics, State University of Campinas, SP, Brazil.

A novel theoretical expression for the relaxation time of magnetic nanoparticles with dipolar interactions is derived from Kramers’ theory, extending the Boltzmann–Gibbs framework to incorporate Tsallis statistics. The model provides, for the first time, a unified description of magnetic relaxation from weakly to strongly interacting regimes, culminating in a spin-glass transition. It accounts for both the decrease and increase of the relaxation time with growing dipolar coupling, a long-standing problem in nanoparticle magnetism, as classical phenomenological models fail to elucidate this transition. This result also offers an innovative interpretation of the cut-off temperature, $T_{cut-off}$, as a spin glass transition under the Tsallis distribution framework within the context of Néel–Brown’s relaxation theory, thereby contributing to ongoing scientific discussions regarding this phenomenon.

I. ARTICLE TEXT

A. Introduction

The study of nanomagnetism in single domain magnetic-nanoparticles (MNPs) began with Néel’s, further advanced by Brown and other key contributors [1–9]. The magnetic moment vector of a MNP is determined by its composition, structure, and temperature, while its orientation is affected by crystalline anisotropy, magnetostatic, and external fields, including interactions with other MNPs. Néel [10] predicted that when thermal agitation $k_B T$) equals the energy required to reverse an MNP’s magnetic moment (μ), its magnetization changes continuously. Delays in magnetization due to external magnetic field changes (H_{ext}) are termed the ”after effect” or ”Néel relaxation time” for MNPs. When the energy barrier $\Delta V(\theta, \phi) = K(\theta, \phi)\nu$ (with $K(\theta, \phi)$ the anisotropy energy density, (θ, ϕ) the anisotropy directions, and ν the MNP volume) is smaller than $k_B T$, the magnetic moments μ of the MNPs are governed by the reversal relaxation time τ [7]. Néel derived τ , the decay factor for the remanent magnetization $M_r(t) = M_s \exp(-\frac{t}{\tau})$, where M_s is the saturation magnetization. For single-domain particles, τ follows the Arrhenius–Néel law $\tau = \tau_0 \exp\left(\frac{K\nu}{k_B T}\right)$ with τ_0 being the material-dependent attempt time (characteristic microscopic timescale). Conversely, Kramers’ theory [11] describes the thermal activation of a particle, such as an MNP in a two-level potential well, by thermal fluctuations from the environment. The particle reaches equilibrium under the Boltzmann–Gibbs (BG) distribution, but may occasionally acquire sufficient energy to cross the potential barrier, temporarily altering the local BG distribution; hence, the core assumption of Kramers’ theory is that the system follows BG statistics. In the framework

of Kramers’ theory, the escape rate (Γ) is expressed as $\Gamma = \Lambda e^{-\frac{\Delta V}{k_B T}}$, where ΔV is the energy barrier. A primary emphasis within this theoretical context is the determination of the prefactor Λ , which is essential for a comprehensive understanding of the relaxation phenomenon. Furthermore, Kramers’ theory facilitates the comprehensive derivation of the phenomenological Néel approximation. Key reviews of Kramers’ theory are available in the works of P. Hänggi et al., and by W. T. Coffey and Yuri P. Kalmykov [12, 13]. Brown *et al.* formulated a dynamic theory to examine both statistical equilibrium and transitional states concerning Brownian motion [4, 14, 15]. This involves the Langevin equation, which includes a random force from thermal fluctuations and Landau–Gilbert–Brown (LGB) equation. In particular, the Fokker–Planck equation for the LGB model was derived under the assumption of a Boltzmann–Gibbs (BG) energy distribution, expressed as $p(E) \sim e^{-\beta E}$, for particles confined within potential wells [4], where β is the inverse thermal energy (usually defined as the inverse temperature parameter). A unit sphere model was employed to represent the orientation of magnetic moments, whereby points on the surface of the sphere correspond to the position of unit vectors. Consequently, the LGB equation [15] was reformulated to incorporate a stochastic field $\mathbf{h}(t)$, which arises due to thermal fluctuations [14].

Dipolar interactions are inherent to any real MNP systems and are critical in determining the magnetic properties of these systems under the influence of an external magnetic field.[16–21]. Furthermore, empirical evidence suggests the occurrence of spin glass (SG) or SG-like states, which are marked by a shift from Néel–Brown-type superparamagnetic relaxation to a power-law behavior characteristic of SG systems [22–26]. These states, which appear to result from interactions between MNPs, remain challenging to explain with current theoretical models. Stoner and Wohlfarth suggested the use of the Vogel–Fulcher (VF) law in magnetic interacting systems in the context of Spin-Glass [27], which later became known as the T^* model [28]. In the T^* context, $k_B T$ in the Néel relaxation time equation is replaced with

* dmuraca@unicamp.br; <https://sites.ifi.unicamp.br/dmuraca/en/>; Also corresponding researcher of the National Scientific and Technical Research Council (CONICET), Argentina.

$k_B(T - T^*)$, incorporating dipolar interactions and the concept of an apparent magnetic moment at the freezing temperature T^* proportional to a mean square dipolar field $\langle B_i^2 \rangle$. Dormann *et al.* [29] introduced a model (DBF) where the dipolar interaction among neighboring particles modulates the energy barrier, yielding $\Delta E = E_a + E_i$, where E_i accounts for interparticle coupling. Subsequently, Mørup and Tronc (MT) suggested that interactions induce a random dipolar field, resulting in a reduction of the effective energy barrier [16]. Both the DBF and VF models forecast an increase in the energy barrier as the interaction strength increases, while the MT model anticipates a decrease in the energy barrier under weak interaction conditions. These models are obtained from the traditional Néel–Brown relaxation time expression derived from Kramers’ theory. They integrate interactions either through the modulation of energy barriers ΔE , resulting in an increase (as in the DBF model) or a decrease (as in the MT model), or through the modification of the thermal fluctuation parameter $k_B T$, as executed in the VF law or T^* model.

When interparticle interactions are negligible, the relaxation of MNPs follows the standard Néel–Brown law as derived from escape-rate theory: a single energy barrier ΔE (or a narrow distribution of barriers) leads to a narrow distribution of relaxation times and an Arrhenius-type plot that yields physically reasonable values for the anisotropy constant and the prefactor τ_0 . Additionally, the introduction of corrections via the VF, MT, and DBF methodologies could potentially bring the phenomenological results into closer agreement with the experimental observables in weak interaction systems. The influence of dipolar interactions on the magnetism of MNPs has been extensively investigated using models such as Landau–Lifshitz–Gilbert simulations and mean-field theory, aiming to provide key insights into dipolar coupling and its impact on relaxation dynamics [30–38]. Stochastic and Monte Carlo simulations have further been employed to elucidate the transition from Arrhenius-type relaxation to superspin-glass behavior [33, 39–41]. In addition, mesoscopic and statistical approaches have been proposed to account for local variations in effective parameters—such as inverse temperature—arising from interparticle interactions and spatial heterogeneity [30, 41–43].

While the mentioned theoretical/phenomenological approaches account for interactions in different ways, they all remain constrained by the Néel–Brown framework, which assumes a BG distribution for the system’s energy, even in the presence of significant interparticle interactions. However, as correlations among magnetic moments increase, the BG statistical framework may fail to accurately characterize the system’s energy distribution. This inadequacy stems from fluctuations in the inverse temperature parameter β . Locally, within spatial “cells,” β can be seen as nearly constant, making the energy distribution in each cell follow the usual Boltzmann factor $e^{-\beta E}$, with E representing the effective energy. Address-

ing fluctuations requires averaging over spatial-temporal variations of β , producing two statistical contributions: one from the distribution of β and another from the local Boltzmann factor $e^{-\beta E}$, as described in *superstatistics* by Beck and Cohen [44]. For moderate to strong interactions, the inadequacy of the Néel–Brown model becomes evident, as it fails to generate valid physical parameters through straightforward barrier adjustments, as initially observed by Dormann [45]. In this regime, nanoparticles can be characterized as *superspins* within a strongly correlated ensemble, manifesting glass-like characteristics, magnetic aging, memory effects, and critical slowing down, which closely resemble the dynamics observed in spin glasses [46–48]. Hence, one often applies a spin-glass critical dynamics law, valid only in the vicinity of the glass transition, i.e. $T \rightarrow T_g$, $\tau = \tau^* \left(\frac{T_g}{T - T_g} \right)^{z\nu}$, where $z\nu$ is a critical exponent, and τ^* is the flip time of a single spin, whereas for MNPs it corresponds to the flip time of the magnetic moments. This letter introduces a generalized theory based on Brown’s formalism for interacting MNP systems, extending the Boltzmann–Gibbs framework to the *Tsallis statistics*, as first proposed in 1988 [49]. Within this framework, entropy assumes a non-extensive nature, resulting in the emergence of *non-extensive statistical mechanics*. This leads to a generalized energy distribution, referred to as the q -distribution: $p(E) \propto e_q^{-\beta'_q E} = [1 - (1 - q)\beta'_q E]^{\frac{1}{1-q}}$. Here, q serves as the entropic index, which quantifies the degree of non-extensivity and links microscopic fluctuations that are difficult to account for to the emergent macroscopic statistics. Specifically, $q = 1$ retrieves the conventional Boltzmann–Gibbs statistics, whereas $q \neq 1$ accounts for deviations engendered by correlations, memory effects, or long-range interactions. This formalism has proven successful in describing various complex systems [50–55].

B. Theory and Results

To account for interparticle interactions, we consider Brown’s formalism of the unitary sphere model, where an MNP magnetic moment \mathbf{u} is represented by a point with angular coordinates (θ, ϕ) . This unit vector’s behavior follows the stochastic (LGB) equation:

$$\dot{\mathbf{u}}(t) = \gamma \left[\left(\mathbf{H}(t) + \mathbf{h} - \frac{\alpha}{\gamma} \dot{\mathbf{u}}(t) \right) \times \mathbf{u}(t) \right], \quad (1)$$

where α is the damping constant, γ is the gyromagnetic ratio, and $\mathbf{H}(t)$ and $\mathbf{h}(t)$ are the applied and random magnetic fields, respectively. Assuming the continuity equation for the probability density function $W(\theta, \phi, t)$ on the unit sphere, a corresponding Fokker–Planck equation can be derived. Contrary to the traditional methodology, we do *not* postulate an isotropic diffusion coefficient in Fick’s law $J_{diff} = -k' \nabla W$ due to the induced fluctuations in interactions, as previously elaborated.

Under conditions of uniaxial symmetry, the Fokker–Planck equation takes on the following form:

$$\frac{\partial W}{\partial t} = \frac{h'}{\sin \theta} \frac{\partial}{\partial \theta} \left(\sin \theta \frac{dV(\theta)}{d\theta} W \right) + \frac{1}{\sin \theta} \frac{\partial}{\partial \theta} \left(\sin \theta k' \frac{\partial W}{\partial \theta} \right), \quad (2)$$

where $h' = \lambda/(\alpha + \alpha^{-1})\mu_0 M_s$ reflects the deterministic drift component, with μ_0 being Bohr's magneton and M_s the saturation magnetization, k' is the probability of anisotropic diffusion resulting from spatio-temporal fluctuations in the system, and $V(\theta)$ is the potential energy, uniaxial in our case. By considering the Tsallis energy distribution (see IV) as the stationary solution of Eq. 2 given by $W_0 = e_q^{-\beta'_q(V(\theta)-V(\theta_0))}/Z$, where $V(\theta_0)$ is the global minimum of potential energy, Z represents the partition function, and β'_q denotes the Lagrange multiplier of the internal energy constraint, the diffusion coefficient k' can be ascertained, leading to:

$$k' = h' \frac{Z^{1-q}}{\beta'_q} W_0^{1-q}. \quad (3)$$

From the Tsallis–Mendes–Plastino formulation [56], the β'_q parameter respects the following self-consistent relation:

$$\beta'_q = \frac{\chi_q^{-1}}{k_B \left(T + (1-q) \frac{U_q}{\chi_q k_B} \right)} = \frac{\chi_q^{-1}}{k_B (T \pm T^*)}, \quad (4)$$

where $+$ or $-$ signifies $q < 1$ or $q > 1$, respectively; χ_q represents a normalization constant defined as $\chi_q = 2\pi \int_0^\pi W_0^q \sin(\theta) d\theta$; and U_q signifies the q -expectation value of the internal energy defined as:

$$U_q = \frac{2\pi \int_0^\pi W_0^q V(\theta) \sin(\theta) d\theta}{\chi_q},$$

and where, for convenience, the temperature T^* was defined as:

$$T^* = \frac{|1-q| U_q}{k_B \chi_q}. \quad (5)$$

The equation 2 can be reformulated appropriately to determine the Fokker-Planck operator L_{fp} and address the mean first passage time problem for the interval (θ_i, θ_c) , thereby yielding the reversal time for $q < 2$:

$$\langle T_1 \rangle(\theta_i) = 2\tau_N \int_{\theta_i}^{\theta_C} \frac{(1 - (1-q)\beta'_q V(\theta))^{\frac{2-q}{1-q}}}{\sin(\theta)} d\theta \times \int_{\theta_i}^{\theta} (1 - (1-q)\beta'_q V(\theta'))^{\frac{1}{1-q}} \sin(\theta') d\theta' \quad (6)$$

where $\tau_N = \frac{\beta'_q}{2h'}$ is a characteristic time constant. In the high-barrier limit, a saddle point approximation can be

made for the potential $V(\theta) = K\nu \sin^2(\theta)$, where K is the effective anisotropy constant and ν is the particle's volume. Because most of the contributions of the integrals in Eq 6 come from the points near (θ_i, θ_C) , when θ_i is one of the wells, i.e., $V(\theta_i) = 0$, and θ_C is the maximum of the potential, the reversal time asymptotically approaches:

$$\tau_i = \tau_0 (1 - (1-q)\beta'_q V(\theta_C))^{\frac{q-3}{2(1-q)}}, \quad (7)$$

where τ_0 is defined as:

$$\tau_0 = \frac{\tau_N \sqrt{2} C_1}{\sin(\theta_C) (\beta'_q)^{3/2} V''(\theta_i) (2-q)} \cdot \frac{1}{\sqrt{|V''(\theta_C)|}}, \quad (8)$$

with $V''(\theta)$ being $d^2V(\theta)/d\theta^2$ and the constant C_1 is given by:

$$C_1 = \begin{cases} \frac{\sqrt{\pi} \Gamma(\frac{1}{2} + \frac{1}{1-q})}{\sqrt{1-q} \Gamma(\frac{q-2}{q-1})}, & \text{if } q < 1, \\ \sqrt{\pi}, & \text{if } q = 1, \\ \frac{\sqrt{\pi} \Gamma(\frac{1}{q-1})}{\sqrt{q-1} \Gamma(\frac{1}{2} + \frac{1}{q-1})}, & \text{if } q > 1. \end{cases} \quad (9)$$

For $q = 1$, Eq . (7) matches Brown's classical asymptotic formula. The same result given by this equation can be obtained by accounting for deviations from normal diffusion due to interactions through a generalized form of Fick's law $J = -k' \nabla W^\nu$ extensively studied in nonextensive statistical mechanics, resulting in Tsallis energy distributions as stationary solutions in porous media diffusion processes [57]. In accordance with these diffusion processes, $q > 1$ denotes superdiffusive behavior, whereas $q < 1$ pertains to subdiffusion [58, 59]. Normal diffusion is recovered in the limit $q = 1$. By comparing with diffusion processes, our results, as presented in Eq. 7, exhibit an analogy with the generalized theory of the Arrhenius law specific to porous media, as proposed by Lenzi *et al.* [60].

In particular, the Tsallis formalism for $q < 1$ imposes an abrupt cut-off to ensure the positivity of the distribution, i.e. $(1 - (1-q)\beta'_q V(\theta_C)) > 0$. From this condition, a cut-off temperature $T_{\text{cut-off}}$ can be defined, below which the probability distribution becomes identically zero:

$$T_{\text{cut-off}} = \frac{|1-q|}{k_B \chi_q} (\Delta V - U_q). \quad (10)$$

where $\Delta V = V(\theta_C)$ is the energy barrier. Although $T_{\text{cut-off}}$ was derived when $q < 1$, it can be employed to reformulate Eq. (9), resulting in three distinct regimes:

$$\tau = \begin{cases} \tau_0 \left(\frac{T + T^*}{T - T_{\text{cut-off}}} \right)^{\frac{3-q}{2(1-q)}}, & q < 1, \\ \tau_0 \exp(K\nu/(k_B T)), & q = 1, \\ \tau_0 \left(\frac{T - T^*}{T + T_{\text{cut-off}}} \right)^{\frac{3-q}{2(1-q)}}, & q > 1, \end{cases} \quad (11)$$

For $q < 1$, the relaxation time τ diverges at $T = T_{\text{cut-off}}$ due to the abrupt energy cut-off, leading to thermodynamic freezing. For $q = 1$, the standard Boltzmann–Gibbs statistics is recovered, with τ following a classical Néel-Brown behavior. For $q > 1$, the distribution acquires a long power-law tail instead of a cut-off and remains positive across all accessible energy levels. In this case, no such transition temperature exists, and consequently, no divergence of τ occurs.

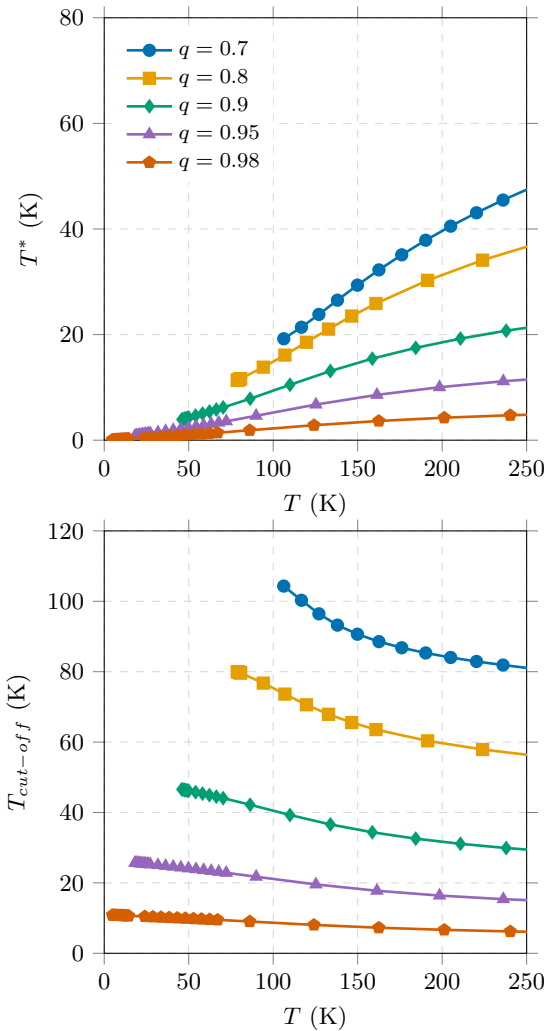


FIG. 1: (first) T^* vs temperature T ; (second) $T_{\text{cut-off}}$ vs temperature for an energy barrier $\Delta V/k_B = 555\text{K}$ and different values of q .

Figure 1 demonstrates the behavior of the temperatures T^* (and $T_{\text{cut-off}}$) as a function of temperature. Figure 1 (left) shows T^* increase (with internal energy (U_q)) as temperature increases, while q is constant. It also increases as q decreases at a fixed temperature, showing a direct correlation between T^* and interparticle interactions. Figure 1 (right) shows that $T_{\text{cut-off}}$ decreases as temperature increases. The possible limit value of $T_{\text{cut-off}}$, linked to temperature transition, increases with

MNPs interaction strength. Hence, the strength of MNPs interaction determines both T^* , related to internal energy, and the transition temperature $T_{\text{cut-off}}$.

For a more comprehensive understanding of $T_{\text{cut-off}}$, Figure 2 illustrates the relationship between $T_{\text{cut-off}}$ and the temperature T , as functions of β'_q (for the arbitrarily selected value of $q = 0.7$, to illustrate a representative example of the transition temperature expressed in Eq. (4)). In particular, the normalization constant χ_q and the q -expectation value U_q are q -weighted statistical averages; as such, they depend on the occupation probabilities of the microstates and therefore vary with the thermodynamic conditions (temperature), inducing corresponding changes in β'_q . When the temperature reaches $T = T_{\text{cut-off}}$, a transition from a superparamagnetic to a glassy-like state occurs, in which the system is thermodynamically frozen in a non-ergodic state. In a dense system of strongly interacting MNPs, the combination of positional disorder and frustrating dipolar interactions creates a rugged energy landscape that dictates its complex critical dynamics. Below the glass temperature, this system exhibits broken ergodicity and is confined to a local energy valley. The Tsallis statistics ($q < 1$) could effectively model this, with a cut-off condition limiting maximum energy, representing the barrier that keeps the MNPs system in its valley. By assigning zero probability to higher energy states, the $q < 1$ framework captures the system's confinement and non-ergodic nature.

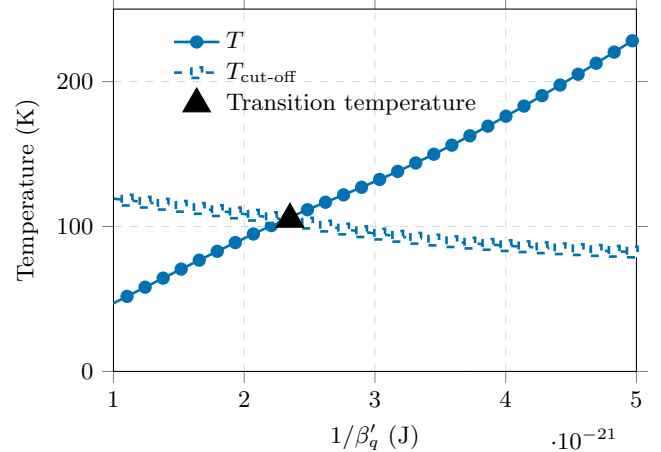


FIG. 2: Temperatures T (solid line) and $T_{\text{cut-off}}$ (dashed line) as a function of $1/\beta'_q$ for $q=0.7$, indicating the transition temperature where $T = T_{\text{cut-off}}$.

Figure 3 shows the relaxation time as a function of the inverse of temperature, considering a system with an energy barrier of $\Delta V/k_B = 555\text{K}$, for ultradiluted 4.7 nm $\gamma\text{-Fe}_2\text{O}_3$ MNP's, as reported by Dormann *et al.* with different concentrations [24]. The Eq. (6) was numerically integrated (symbols) to represent the expected behavior of the relaxation time, which was subsequently compared to the high barrier approximation using Eq. 11 (lines). A transition from sub-diffusive to super-diffusive behav-

ior can be observed under the condition $q = 1$, where the model captures classical Néel-Brown non-interacting behavior. Generally, for $q < 1$ (sub-diffusive), reducing q makes the system resemble a strongly interacting nanoparticle ensemble, where the relaxation time increases as q decreases (interactions strengthen) and diverges at a finite critical temperature. The particle size, geometry, and spatial arrangement of MNPs should also affect q . Even with similar mean separations, variations in local ordering or magnetic anisotropy can lead to different levels of nonextensivity. A thorough understanding of how these structural factors affect q needs further experimental, simulation, and/or theoretical study.

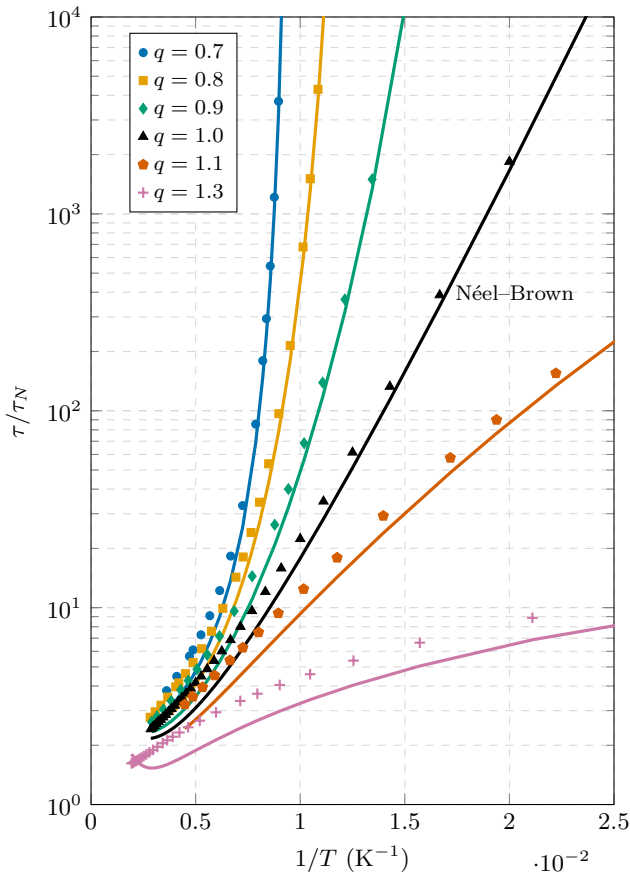


FIG. 3: A comparative analysis between the numerically calculated relaxation time, Eq (6) (symbols) and the asymptotic approximation, Eq. 11 (lines), for various values of the parameter q . The approximation is more accurate for lower temperatures in the high barrier limit.

In the super-diffusive scenario ($q > 1$), a reduction in relaxation time is observed as q increases. Reports on super-diffusive regimes in MNPs systems are scarce, indicating that this behavior is not universal but occurs under specific spatial configurations, such as chain-like assemblies, for example [16, 61, 62]. These create inhomogeneous dipolar fields, leading to collective magne-

ization dynamics predicted by nonextensive statistical mechanics. Similar super-diffusion appears in other complex systems only in certain microstructural or dynamic settings. Thus, in the Tsallis framework, $q > 1$ behavior signals specific correlated states, not a general system trait.

C. Application of the theory

The applicability of the model was based on classical and well-recognized literature reported on magnetic interaction strength and diverse types of collective behaviors [24, 26]. Equation (11) was used to analyze the reported data and to correlate the fitted parameters with theoretical predictions.

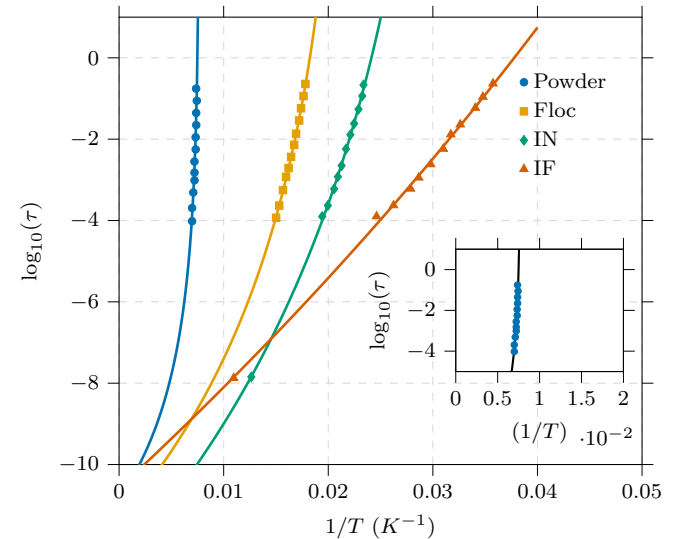


FIG. 4: Relaxation time τ as a function of inverse temperature $1/T$ for samples with increasing concentrations IF, IN, Floc for the conglomerated sample and for a Powder sample. The lines indicate the fit from Eq (11). The relaxation time increases with interaction strength, indicating slower dynamics in more strongly interacting assemblies. An inset displays a fit to the spin-glass equation for the Powder sample yielding $\tau^* = 10^{-10 \pm 2}$ s, $z\nu = 7 \pm 3$ and $T_g = 130 \pm 4$ K. Data reproduced from Fig. 1 of Dormann *et al.* [24].

TABLE I: Parameters obtained from fitting the Eq (11)

Sample	$\log_{10}(\tau_0)$	$T_{cut-off}$ [K]	T^* [K]	q
Powder	-11 ± 3	130 ± 4	20	0.8 ± 0.1
Floc	-11.3 ± 0.5	45 ± 2	2.8	0.93 ± 0.01
IN	-12.4 ± 0.5	30.1 ± 0.9	1.0	0.954 ± 0.003
IF	-10.5 ± 0.2	7 ± 2	0.1	0.986 ± 0.005

Figure 4 presents the relaxation time of four distinct samples with variable interparticle center-to-center distances d_{cc} of $\gamma\text{-Fe}_2\text{O}_3$ MNPs (diameter $D = 4.7$ nm) as

investigated by Dormann *et al.* [24]: $d_{cc} \approx 21$ nm (long-range dispersed 'isolated far' particles IF), 7.3 nm (short-range dispersed 'isolated near' particles IN) and 6.8 nm for large conglomerates (clustered 'flocculated' particles Floc). The dry powder sample has the d_{cc} slightly larger than D . The parameters derived from the analyses using Eq 11 are enumerated in Table I. The most diluted sample (IF) is the closest to the Néel–Brown ideal behavior. As the interaction strength increases, the relaxation curves develop a slight curvature and the relaxation time grows. From our analysis q values progressively deviate from unity (with $q < 1$) as the interaction strength increases and the magnetic correlation increases. When particles are brought closer, dipolar interactions grow and deviations from Boltzmann–Gibbs behavior are observed, as predicted. The higher uncertainty observed in the powder sample could be attributed to exchange-coupling interactions between the particles. The fitted $T_{\text{cut-off}}$ rises with increasing interaction strength, consistent with a higher temperature for the onset of glassy dynamics in more strongly interacting assemblies. However, the fitted $T_{\text{cut-off}}$ values lie above the theoretical prediction obtained using the same energy barrier for all samples $\Delta V/k_B = 555$ K (the value found by Dormann *et al.* for the ultra-dilute IF sample), as shown in Fig. 1. This discrepancy indicates that the effective energy barrier is progressively underestimated when interactions grow. Dormann *et al.* attributed the barrier corrections found for IN and Floc samples using the (DBF) model to changes in the surface anisotropy induced by interactions: as interparticle coupling alters the magnetostatic state of surface spins, the effective barrier experienced by the moments is modified. In short, increasing interaction strength appears to raise the effective energy barrier, which explains why the theoretical curve with similar q 's computed with the IF value $\Delta V/k_B = 555$ K underestimates the observed $T_{\text{cut-off}}$. The pre-factor τ_0 lies in the expected range for MNPs (typically $\sim 10^{-12}\text{--}10^{-9}$ s). For comparative purposes, the inset of Fig. 4 shows a fit using the classical spin-glass critical law ($\tau = \tau^*(T_g/(T - T_g)^{z\nu})$) (as applied by Dormann *et al.*) to the Powder sample, yielding $T_g = 130 \pm 4$ K, in agreement with the $T_{\text{cut-off}}$ predicted from the Tsallis formalism. Dormann *et al.* also observed independent signatures of collective spin-glass-like freezing at this temperature: (i) an increase of the nonlinear susceptibility (extracted from the low-field expansion of MNPs magnetization upon cooling toward $T_g \approx 130$ K) and (ii) pronounced waiting-time (aging) dependence behavior in the ZFC relaxation for the powder sample for the temperatures (80K, 90K, and 118K), features that are much weaker or absent in the more dilute samples.

In Figure 5, results reported by C. Djurberg *et al.* [26] are presented, with analyses using Eq. (11). Specifically, C. Djurberg *et al.* examined two different samples of ultrafine Fe–C particles characterized by a median volume $V = 5.3 \times 10^{-26}$ m³ (diameter $d \approx 4.7$ nm) with varying carbon volume concentrations: one sample at 5% and the

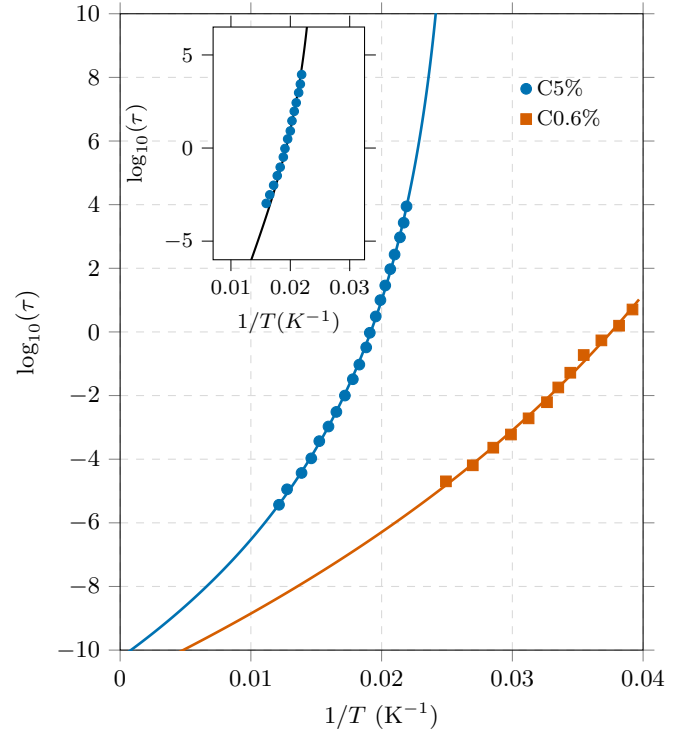


FIG. 5: Relaxation time versus inverse temperature for the samples C5% and C0.6%. The main plot shows fits to Eq. (11). The inset displays a fit to the spin-glass equation for the C5% sample, yielding the parameters $\tau^* = 10^{-6.2 \pm 0.3}$ s, $T_g = 40 \pm 2$ K, and $z\nu = 15 \pm 3$. Data reproduced from Fig. 2 of Djurberg *et al.* [26].

other at 0.6%. Results obtained from fitting Eq. (11) are summarized in Table II. As the concentration increases, the entropic index q once more deviates from 1 (decreasing), consistent with increased interaction effects. In the case of the 0.6% concentration sample, C. Djurberg *et al.* suggested the potential occurrence of particle agglomeration. This phenomenon might elucidate the observed deviation from ideal superparamagnetic linearity and corresponds with the deduced entropic index q , when taking into account the model proposed herein. For comparison, the spin-glass critical law was used to fit the original data and temperature range chosen by the authors in [26], but the fit is unsatisfactory, as shown in the inset of Fig. 5. Narrowing the fit to 45–55 K improves agreement, bringing data closer to the glass transition temperature T_g . The shorter-range fit yields $\tau^* = 10^{-6.2 \pm 0.3}$ s, $T_g = 37 \pm 2$ K, $z\nu = 15 \pm 3$. Regardless of the selected interval, the derived T_g values exhibit a strong agreement with the value extracted for $T_{\text{cut-off}}$ from fitting across the complete 45–85 K range using Eq. (11), as illustrated in Table II. Additionally, C. Djurberg *et al.* reported magnetic aging in the C5% sample at $T = 40$ K and $T = 30$ K, whereas no aging was observed for the time window of the experiment at $T = 50$ K. This finding supports the existence of the superspin-glass behavior for

this composition lying in the 30-40 K range.

TABLE II: Parameters obtained from fitting the Eq (11)

Sample	$\log_{10}(\tau_0)$	$T_{cut-off}$ [K]	T^* [K]	q
C5%	-10.3 \pm 0.2	38.4 \pm 0.4	2.5	0.939 \pm 0.002
C0.6%	-10.9 \pm 0.7	15 \pm 2	0.8	0.96 \pm 0.01

In conclusion, the utilization of Brown's framework to model the magnetic behavior of MNPs with dipolar interactions provides a meaningful contribution to understanding the transition from weakly to strongly interacting magnetic systems, extending to spin-glass transitions. When interparticle interactions are negligible, the relaxation of magnetic nanoparticles follows the standard Néel–Brown law as derived from escape-rate theory: a single energy barrier ΔE (or a narrow distribution of barriers) leads to a narrow distribution of relaxation times and an Arrhenius-type plot that yields physically reasonable values for the anisotropy constant and the prefactor τ_0 . As interactions become weak but nonzero, for example in dilute dispersions, the Néel–Brown framework could still represent experimental results with minor modifications: dipolar or exchange coupling shifts the effective barrier up (DBF) or down (MT) without altering the fundamental Boltzmann-law kinetics, or can be absorbed into a mean-field correction (VF or T^* models) that effectively modifies the thermal energy scale $k_B T$. Hence, existing theories and models provide a valuable approximation for the behavior of MNPs with weak

magnetic interactions, but they fail to clarify the transition from weak to strong interaction behaviors. The DBF, MT, and VF (or T^*) models assume thermodynamic equilibrium under the Boltzmann-Gibbs distribution, which holds only for non-interacting systems. This assumption fails for dipole-coupled MNPs ensembles, where long-range correlations and collective interactions make the system's entropy non-extensive. The theory presented here not only predicts the spin-glass transition temperature for these systems but also offers insights into both the increased and decreased relaxation times observed experimentally, from weak to strong interactions. Additionally, it provides an innovative interpretation of the cut-off temperature, $T_{cut-off}$, as a spin-glass transition, under the Tsallis distribution framework, thus advancing the ongoing scientific discussions surrounding this phenomenon.

II. ACKNOWLEDGMENTS

This study was mainly supported and performed under the auspices of the São Paulo Research Foundation (FAPESP) under Grant No. 2024/03819-5 and 24/00998-6. We express our gratitude to Prof. Fernando Fabris.

III. DATA AVAILABILITY

The data are available from the corresponding author upon a reasonable request.

-
- [1] L. Néel, Théorie du traînage magnétique des ferromagnétiques en grains fins avec applications aux terres cuites, *Ann. Geophys.* **5**, 99 (1949).
- [2] L. Néel, Théorie du traînage magnétique des substances massives dans le domaine de Rayleigh, *Journal de Physique et le Radium* **11**, 49 (1950).
- [3] W. Brown, Thermal fluctuations of fine ferromagnetic particles, *IEEE Transactions on Magnetics* **15**, 1196 (1979).
- [4] W. F. Brown, Thermal fluctuations of a single-domain particle, *Physical Review* **130**, 1677 (1963).
- [5] A. Aharoni, Relaxation processes in small particles, in *Magnetic Properties of Fine Particles*, North-Holland Delta Series, edited by J. Dormann and D. Fiorani (Elsevier, Amsterdam, 1992) pp. 3–11.
- [6] E. C. Stoner and E. P. Wohlfarth, A mechanism of magnetic hysteresis in heterogeneous alloys, *Philosophical Transactions of the Royal Society of London. Series A, Mathematical and Physical Sciences* **240**, 599 (1948).
- [7] C. P. Bean and J. D. Livingston, Superparamagnetism, *Journal of Applied Physics* **30**, S120 (1959).
- [8] J. L. Dormann, D. Fiorani, and E. Tronc, Magnetic relaxation in fine-particle systems, *Advances in Chemical Physics* **98**, 283 (1997).
- [9] W. T. Coffey, D. S. F. Crothers, J. L. Dormann, P. Y. Kalmykov, E. C. Kennedy, and W. Wernsdorfer, Thermally activated relaxation time of a single domain ferromagnetic particle subjected to a uniform field at an oblique angle to the easy axis: Comparison with experimental observations, *Physical Review Letters* **80**, 5655 (1998).
- [10] L. Néel, Influence des fluctuations thermiques sur l'aimantation de grains ferromagnétiques très fins, *Comptes Rendus Hebdomadaires des Séances De l'Academie des Sciences* **228**, 664 (1949).
- [11] H. Kramers, Brownian motion in a field of force and the diffusion model of chemical reactions, *Physica* **7**, 284 (1940).
- [12] P. Hänggi, P. Talkner, and M. Borkovec, Reaction-rate theory: Fifty years after Kramers, *Rev. Mod. Phys.* **62**, 251 (1990).
- [13] W. T. Coffey, Y. P. Kalmykov, and J. T. Waldron, The Langevin equation: With applications to stochastic problems in physics, chemistry and electrical engineering, World Scientific Series in Contemporary Chemical Physics <https://doi.org/10.1142/5343> (2004).
- [14] W. T. Coffey and Y. P. Kalmykov, Thermal Fluctuations of Magnetic Nanoparticles: Fifty Years After Brown, *Journal of Applied Physics* **112**, 121301 (2012).
- [15] T. L. Gilbert, A phenomenological theory of damping in ferromagnetic materials, *IEEE Transactions on Magnetics* **40**, 3443 (2004).
- [16] S. Mørup and E. Tronc, Superparamagnetic relaxation of weakly interacting particles, *Physical Review Letters* **72**,

- 3278 (1994).
- [17] L. C. Branquinho, M. S. Carrião, A. S. Costa, N. Zufelato, M. H. Sousa, R. Miotto, R. Ivkov, and A. F. Bakuzis, Effect of magnetic dipolar interactions on nanoparticle heating efficiency: Implications for cancer hyperthermia, *Scientific Reports* **3**, 10.1038/srep02887 (2013).
- [18] G. T. Landi, Role of dipolar interaction in magnetic hyperthermia, *Physical Review B* **89**, 014403 (2014).
- [19] O. Moscoso-Londoño, D. Muraca, K. R. Pirota, M. Knobel, P. Tancredi, L. M. Socolovsky, P. M. Zélis, D. F. Coral, U. W. M. B Fernández van Raap, C. D. V. Neu, and C. L. P. de Oliveira, Different approaches to analyze the dipolar interaction effects on diluted and concentrated granular superparamagnetic systems, *Journal of Magnetism and Magnetic Materials* **428**, 105 (2017).
- [20] D. Serantes, M. Pereiro, R. Chantrell, and D. Baldomir, Scaling the effect of the dipolar interactions on the zfc/fc curves of random nanoparticle assemblies, *Journal of Magnetism and Magnetic Materials* **460**, 28 (2018).
- [21] G. F. Goya and M. P. Morales, Field dependence of blocking temperature in magnetite nanoparticles, *Journal of Metastable and Nanocrystalline Materials* **20-21**, 673 (2004).
- [22] S. Mørup, F. Bødker, P. V. Hendriksen, and S. Linderoth, Spin-glass-like ordering of the magnetic moments of interacting nanosized maghemite particles, *Physical Review B* **52**, 287 (1995).
- [23] W. Luo, S. R. Nagel, T. F. Rosenbaum, and R. E. Rosensweig, Dipole interactions with random anisotropy in a frozen ferrofluid, *Physical Review Letters* **67**, 2721 (1991).
- [24] J. Dormann, L. Spinu, E. Tronc, J. Jolivet, F. Lucari, F. D’Orazio, and D. Fiorani, Effect of interparticle interactions on the dynamical properties of γ -Fe₂O₃ nanoparticles, *Journal of Magnetism and Magnetic Materials* **183**, L255 (1998).
- [25] H. Mamiya, I. Nakatani, and T. Furubayashi, Blocking and freezing of magnetic moments for iron nitride fine particle systems, *Physical Review Letters* **80**, 177 (1998).
- [26] C. Djurberg, P. Svedlindh, P. Nordblad, M. F. Hansen, F. Bødker, and S. Mørup, Dynamics of an interacting particle system: Evidence of critical slowing down, *Physical Review Letters* **79**, 5154 (1997).
- [27] S. Shtrikman and E. P. Wohlfarth, The theory of the Vogel–Fulcher law of spin glasses, *Physics Letters A* **85**, 467 (1981).
- [28] P. Allia, M. Coisson, P. Tiberto, F. Vinai, M. Knobel, M. A. Novak, and W. C. Nunes, Granular Cu-Co alloys as interacting superparamagnets, *Physical Review B* **64**, 144420 (2001).
- [29] J. L. Dormann, D. Fiorani, R. Cherkoui, L. Spinu, F. Lucari, F. D’Orazio, E. Tronc, and J. P. Jolivet, A dynamic study of small interacting particles: superparamagnetic model and spin-glass laws, *Journal of Physics C: Solid State Physics* **21**, 2015 (1988).
- [30] A. R. Chalifour, J. C. Davidson, N. R. Anderson, T. M. Crawford, and K. L. Livesey, Magnetic relaxation time for an ensemble of nanoparticles with randomly aligned easy axes: A simple expression, *Physical Review B* **104**, 094433 (2021).
- [31] P. Ilg and M. Kröger, Longest relaxation time versus maximum loss peak in the field-dependent longitudinal dynamics of magnetic nanoparticles, *Physical Review B* **106**, 134433 (2022).
- [32] D. Gallina and G. M. Pastor, Theory of the collective behavior of two-dimensional periodic ensembles of dipole-coupled magnetic nanoparticles, *Physical Review B* **107**, 184407 (2023).
- [33] M. Anand, Magnetisation reversal in two-dimensional ensemble of nanoparticles with positional defects, *Physics: Open Source Preview*, **97**, 10.1007/s12043-023-02669-z (2023).
- [34] J. M. Porro, J. Bodnár, J. Arlegui, P. Marín, and R. Salazar, Magnetization dynamics of weakly interacting sub-100 nm magnetic nanoparticle arrays: effect of dipolar interactions on relaxation times, *Scientific Reports* **9**, 56219 (2019).
- [35] C. Muñoz-Menéndez, D. Serantes, O. Chubykalo-Fesenko, S. Ruta, O. Hovorka, P. Nieves, K. L. Livesey, D. Baldomir, and R. W. Chantrell, Disentangling local heat contributions in interacting magnetic nanoparticles, *Physical Review B* **102**, 214412 (2020).
- [36] P. García-Acevedo, M. A. González-Gómez, A. Arnosa-Prieto, L. de Castro-Alves, Y. Piñeiro, and J. Rivas, Role of dipolar interactions on the determination of the effective magnetic anisotropy in iron oxide nanoparticles, *Advanced Science* **10**, 2203397 (2023).
- [37] P. Torche, C. Muñoz-Menéndez, D. Serantes, D. Baldomir, K. L. Livesey, O. Chubykalo-Fesenko, S. Ruta, R. Chantrell, and O. Hovorka, Thermodynamics of interacting magnetic nanoparticles, *Physical Review B* **101**, 224429 (2020).
- [38] R. E. Camley, Curie-Weiss behavior and the interaction temperature of interacting nanoparticle assemblies, *Physical Review B* **110**, 144440 (2024).
- [39] P. M. Shand, Y. Moua, H. Harms, C. Gorgen, C. J. Cunningham, P. Lukashev, T. E. Kidd, and A. J. Stollenwerk, Hopping crossover and high-temperature superspin glass dynamics in dense nanoparticle systems, *Physical Review B* **109**, 245432 (2024).
- [40] M. Orendáč, S. Lupíková, A. Doroshenko, E. Čižmár, A. Orendáčová, V. Švorčík, O. Lyutakov, D. Fajstav, Z. Kolská, A. Zeleňáková, and D. Peddis, Super spin-glass state in two-dimensional aggregated Fe₃O₄ nanoparticle assemblies, *Physical Review B* **108**, 104423 (2023).
- [41] G. Barrera, P. Allia, and P. Tiberto, Dipolar interactions among magnetite nanoparticles for magnetic hyperthermia: a rate-equation approach, *Nanoscale* **13**, 4103 (2021).
- [42] M. E. Sadat, S. L. Bud’ko, R. C. Ewing, H. Xu, G. M. Pauletti, D. B. Mast, and D. Shi, Effect of dipole interactions on blocking temperature and relaxation dynamics of superparamagnetic iron-oxide nanoparticle systems, *Materials* **16**, 496 (2023).
- [43] D. Peddis, K. N. Trohidou, M. Vasilakaki, G. Margaris, M. Bellusci, F. Varsano, M. Hudl, N. Yaacoub, D. Fiorani, P. Nordblad, and R. Mathieu, Memory and superposition in a superspin glass, *Scientific Reports* **11**, 87345 (2021).
- [44] C. Beck and E. G. D. Cohen, Superstatistics, *Physica A: Statistical Mechanics and its Applications* **322**, 267 (2003).
- [45] J. L. Dormann, D. Fiorani, and E. Tronc, On the models for interparticle interactions in nanoparticle assemblies: comparison with experimental results, *Journal of Magnetism and Magnetic Materials* **202**, 251 (1999).

- [46] Y. Sun, M. B. Salamon, K. Garnier, and R. S. Averback, Memory effects in an interacting magnetic nanoparticle system, *Physical Review Lett.* **91**, 167206 (2003).
- [47] K. Konwar, S. D. Kaushik, D. Sen, and P. Deb, Dynamic spin freezing and magnetic memory effect in ensembles of interacting anisotropic magnetic nanoparticles, *Physical Review B* **102**, 174449 (2020).
- [48] M. Sasaki, P. E. Jönsson, H. Takayama, and H. Mamiya, Aging and memory effects in superparamagnets and superspin glasses, *Physical Review B* **71**, 104405 (2005).
- [49] C. Tsallis, Possible generalization of Boltzmann-Gibbs statistics, *Journal of Statistical Physics* **52**, 479 (1988).
- [50] G. Wilk and Z. Włodarczyk, Interpretation of the nonextensivity parameter q in some applications of tsallis statistics and Lévy distributions, *Physical Review Letters* **84**, 2770 (2000).
- [51] C. Beck, Dynamical foundations of nonextensive statistical mechanics, *Physical Review Letters* **87**, 180601 (2001).
- [52] H. Sakaguchi, Fluctuation-dissipation relation for a langevin model with multiplicative noise, *Journal of Physics Society of Japan.* **70**, 3247 (2001).
- [53] C. Beck, Tsallis statistics and fully developed turbulence, *Physica A* **322**, 267 (2003).
- [54] R. M. Pickup, R. Cywinski, C. Pappas, B. Farago, and P. Fouquet, Generalized spin-glass relaxation, *Physical Review Letters* **102**, 097202 (2009).
- [55] C. Tsallis, J. C. Anjos, and E. P. Borges, Fluxes of cosmic rays: A delicately balanced stationary state, *Physical Letters A* **310**, 372 (2003).
- [56] C. Tsallis, S. R. Mendes, and A. R. Plastino, The role of constraints within generalized nonextensive statistics, *Physica A: Statistical Mechanics and its Applications* **261**, 534 (1998).
- [57] A. R. Plastino and A. Plastino, Non-extensive statistical mechanics and generalized Fokker-Planck equation, *Physica A: Statistical Mechanics and its Applications* **222**, 347 (1995).
- [58] L. Borland, Microscopic dynamics of the nonlinear fokker-planck equation: A phenomenological model, *Physical Review E* **57**, 6634 (1998).
- [59] C. Tsallis and D. J. Bukman, Anomalous diffusion in the presence of external forces: Exact time-dependent solutions and their thermostatistical basis, *Physical Review E* **54**, R2197 (1996).
- [60] E. K. Lenzi, C. Anteneodo, and L. Borland, Escape time in anomalous diffusive media, *Physical Review E* **63**, 051109 (2001).
- [61] O. Iglesias and A. Labarta, Magnetic relaxation in terms of microscopic energy barriers in a model of dipolar interacting nanoparticles, *Physical Review B* **70**, 144401 (2004).
- [62] F. Luis, F. Petroff, J. M. Torres, L. M. García, J. Bartolomé, J. Carrey, and A. Vaurès, Magnetic relaxation of interacting Co clusters: Crossover from two- to three-dimensional lattices, *Physical Review Lett.* **88**, 217205 (2002).

IV. END MATTER

A. Tsallis Statistics

The entropy of a system, as characterized by the Tsallis distribution, is expressed as:

$$S_q = k_B \frac{1 - \sum_i p_i^q}{q - 1},$$

where q denotes the non-extensivity parameter which characterizes the degree of correlation amongst the components of the system. When condition $q \rightarrow 1$ is met, the Boltzmann-Gibbs entropy is recovered, thereby ensuring compatibility with traditional statistical mechanics applicable to extensive systems. This non-extensivity is demonstrated through the property specified in

$$\frac{S_q(A + B)}{k_B} = \frac{S_q(A)}{k_B} + \frac{S_q(B)}{k_B} + (1 - q) \frac{S_q(A)}{k_B} \frac{S_q(B)}{k_B},$$

where $S(A)$ and $S(B)$ represent the entropies of two distinct *independent* systems. The maximization of Tsallis entropy under the constraints given by

$$\sum_i^W p(x) = 1 \quad \text{and} \quad \frac{\sum_{i=1}^W p_i^q E_i}{\sum_{i=1}^W p_i^q} = U_q,$$

where E_i is the energy spectrum and U_q is the q -expectation internal energy, resulting in the generalized probability distribution [56]:

$$p_i = \frac{1}{Z'_q} [1 - (1 - q)\beta'_q E_i]_+^{\frac{1}{1-q}}$$

Here, β'_q is the Lagrange multiplier associated with the energy constraint, related to $\beta = 1/(k_B T)$ via the self-consistent relation:

$$\beta'_q = \frac{\beta}{\sum_{i=1}^W p_i^q + (1 - q)\beta U_q},$$

With the equilibrium distribution $p_i = \frac{e^{-\beta'_q E_i}}{Z'_q}$, the partition function can be determined through:

$$Z'_q \equiv \sum_i^W e^{-\beta'_q E_i}$$

The connection with thermodynamics is established by proving that:

$$\frac{1}{T} = \frac{\partial S_q}{\partial U_q}$$

The condition $[f]_+ = \max\{f, 0\}$ ensures only positive values for the probabilities because sufficiently high energies can produce negative values for the distribution,

thus presenting a cut-off condition for the q-exponential function e_q^x , which can be defined as:

$$e_q^x = \begin{cases} (1 + (1 - q)x)^{1/(1-q)}, & \text{if } 1 + (1 - q)x > 0, \\ 0, & \text{if } q < 1 \text{ and } x < -(1 - q)^{-1}, \end{cases}$$

where the fulfillment of condition $1 + (1 - q)x > 0$ is necessary to assure the existence of the function. When $q > 1$, the domain is constrained to $x \in (-\infty, (q - 1)^{-1})$, and the function diverges as $x \rightarrow (q - 1)^{-1}$ is approached. Conversely, for the case of $q < 1$, the function is defined across all values of x , though it nullifies when $x < -(1 - q)^{-1}$. When approaching the limit of $q \rightarrow 1$, the definition simplifies to the classical exponential form $e_q^x \rightarrow e^x$, ensuring consistency with traditional theory.

B. Analyses Methods

The fits were performed using non-linear least squares. For each dataset T^* was held fixed, chosen from theoretically meaningful values, while the remaining free parameters were determined by the fit. It has been shown in Fig 1 that both T^* and $T_{\text{cut-off}}$ vary with temperature, with a more pronounced variation the further the q parameter is from 1; nevertheless, the range of blocking temperatures is limited, and keeping $T_{\text{cut-off}}$ constant can still provide a good estimate of the collective transition when compared with other methods, particularly for strongly interacting systems close to the critical temperature. When the fitted temperature range lies far from the critical temperature, an underestimation of T_g is expected, as illustrated for q close to 1 in Fig. 1, but the model remains valid within these limits.